Early bird or night owl? Controlling the ultrafast photodynamics of triphenylamine substituted 2,2´:6´,2´´-terpyridine

Anna Maria Maroń, Oliviero Cannelli, Etienne Christophe Socie, Malte Oppermann, Piotr Lodowski, Barbara Machura, Majed Chergui

Electronic Supporting Information

Synthetic procedure and identification of tBuTPAterpy from [1]:

A mixture of 4′-(4-bromophenyl)-2,2′:6′,2″-terpyridine (1.72 g, 4.44 mmol), bis(4-tert-butylphenyl)amine (1.5 g, 5.33 mmol), $Pd(OAc)_2$ (40 mg, 0.18 mmol, 4%-mol), $P(^tBu)_3$ (73 mg, 0.36 mmol, 8%-mol)and NaO^tBu (770 mg, 8 mmol) in 100 mL of anhydrous toluene was heated under reflux for 24 h under argon atmosphere. After this time, the mixture was cooled to room temperature, water (60 mL) was added, and the mixture was stirred for 20 minutes. Then, the mixture was extracted with dichloromethane (30 mL) three times. The combined organic extract was washed with brine and dried with anhydrous Na_2SO_4. The solvent was removed by a rotary evaporator under vacuum. The crude product was purified by column chromatography (silica gel, AcOEt/*n*-hexane/$NH_3 \cdot H_2O$ 75:50:1 v/v) and recrystallized from ethanol, to give **tBuTPAterpy** as a yellow solid (1.64 g, 63%). **^{1}H NMR** (400 MHz, $CDCl_3$) δ 8.73 – 8.71 (m, 4H), 8.66 (d, J = 7.8 Hz, 2H), 7.87 (t, J = 7.7 Hz, 2H), 7.77 (d, J = 8.5 Hz, 2H), 7.36 – 7.28 (m, 6H), 7.15 (d, J = 8.5 Hz, 2H), 7.09 (d, J = 8.4 Hz, 4H), 1.34 (s, 18H). **^{13}C NMR** (100 MHz, $CDCl_3$) δ 156.54, 155.91, 149.88, 149.24, 149.19, 146.34, 144.77, 136.84, 131.03, 128.04, 126.27, 124.55, 123.76, 122.38, 121.38, 118.28, 34.45, 31.57. $C_{41}H_{40}N_4$ (588.79 g/mol) calculated: C, 83.64; H, 6.85; N, 9.52%. Found: C, 83.64; H, 6.95; N, 9.58%.

Stability, photostability and fluence dependence

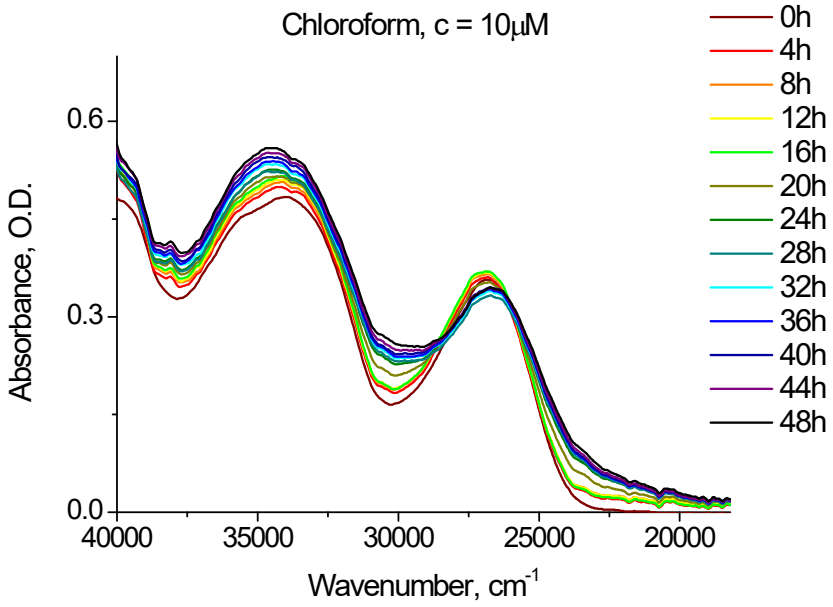

a

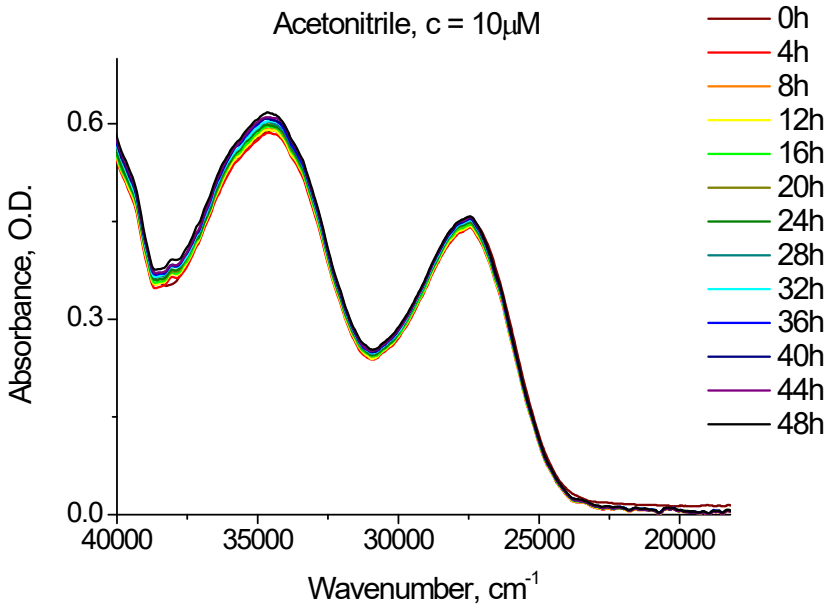

b

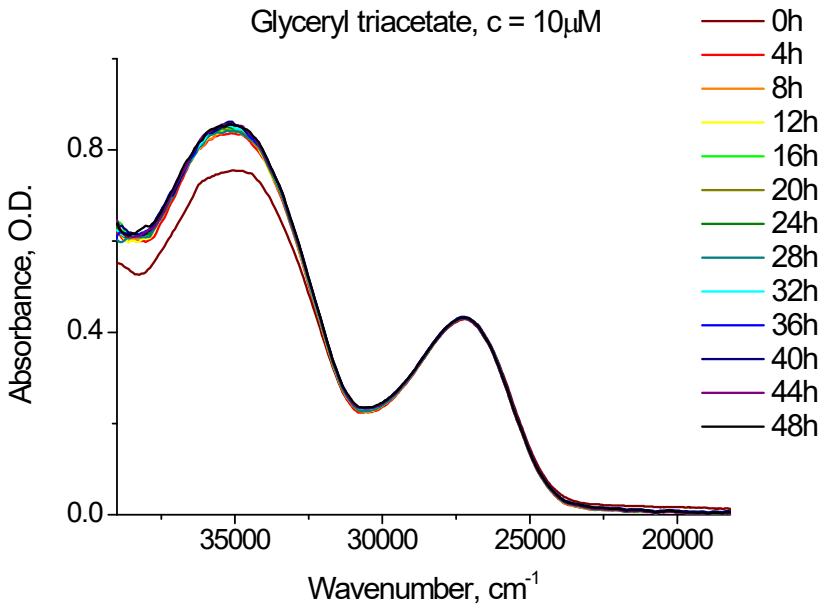

c

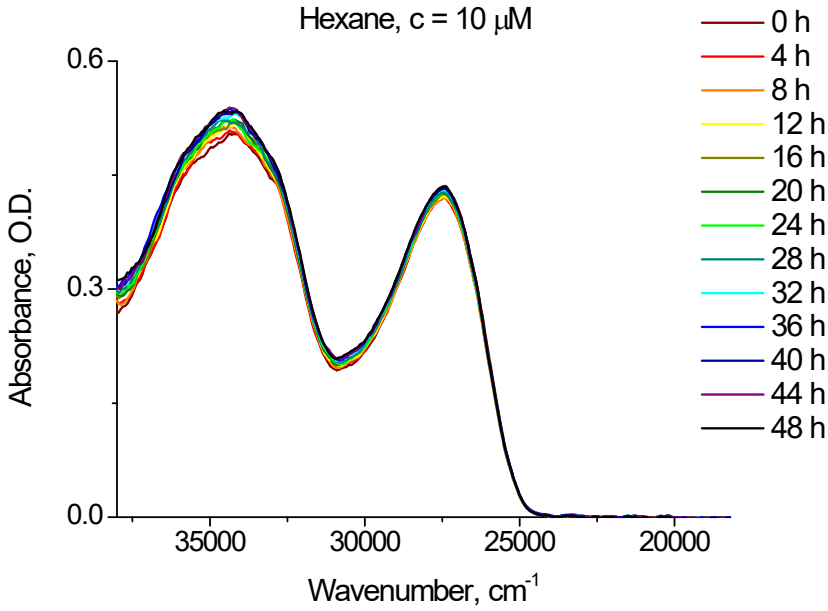

d

Figure S1. Ageing experiments for **tBuTPAterpy** in chloroform (a), acetonitrile (b), glyceryl triacetate (c), hexane (d).

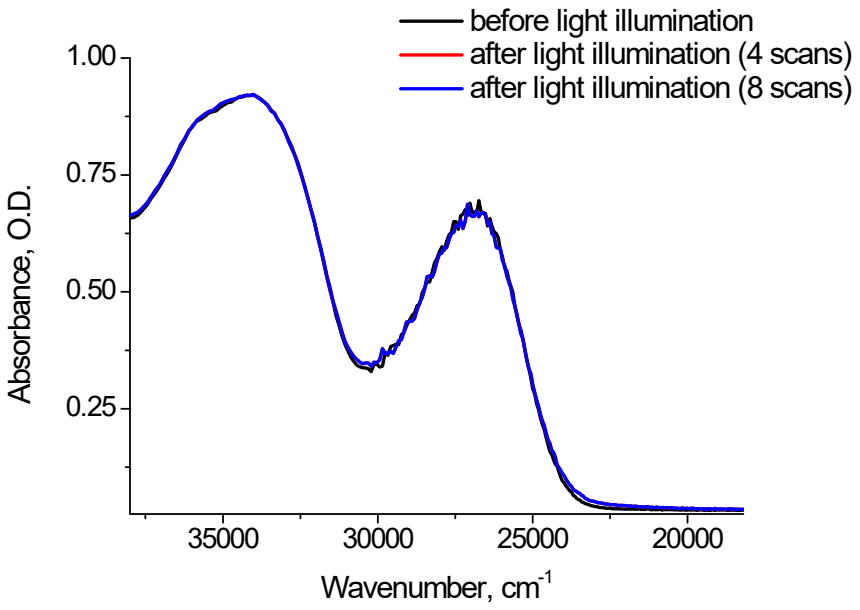
before light illumination
after light illumination (4 scans)
after light illumination (8 scans)
1.00
0.75
0.50
0.25
Absorbance, O.D.
35000
30000
25000
20000
Wavenumber, cm-1

a

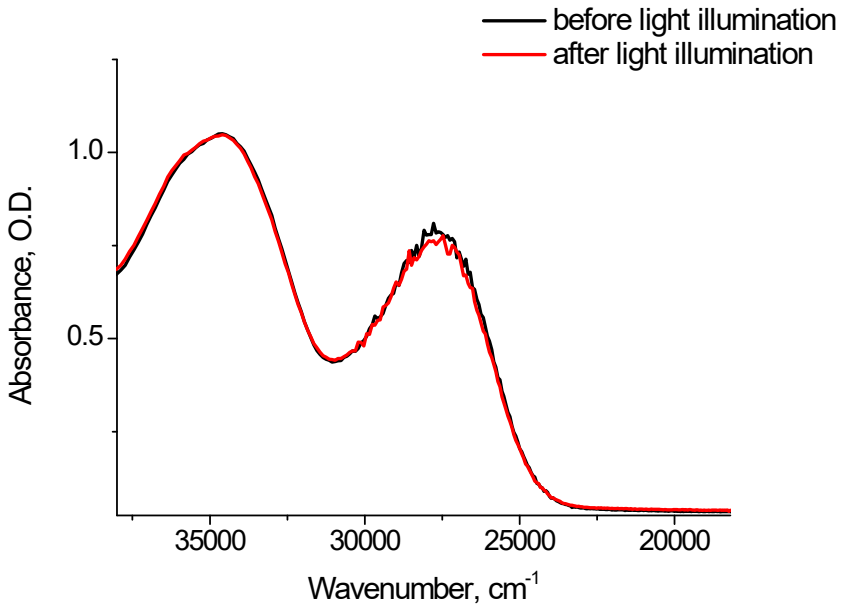
before light illumination
after light illumination
1.0
0.5
Absorbance, O.D.
35000
30000
25000
20000
Wavenumber, cm-1

b

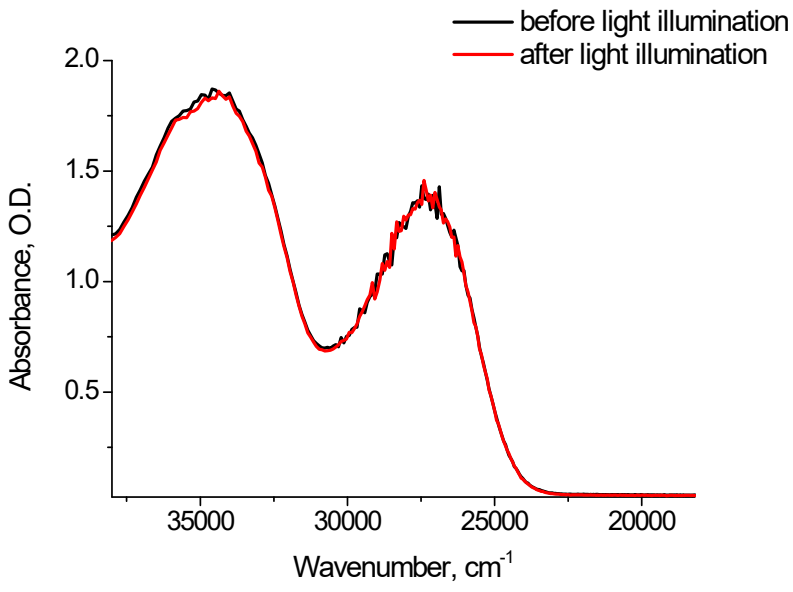

c

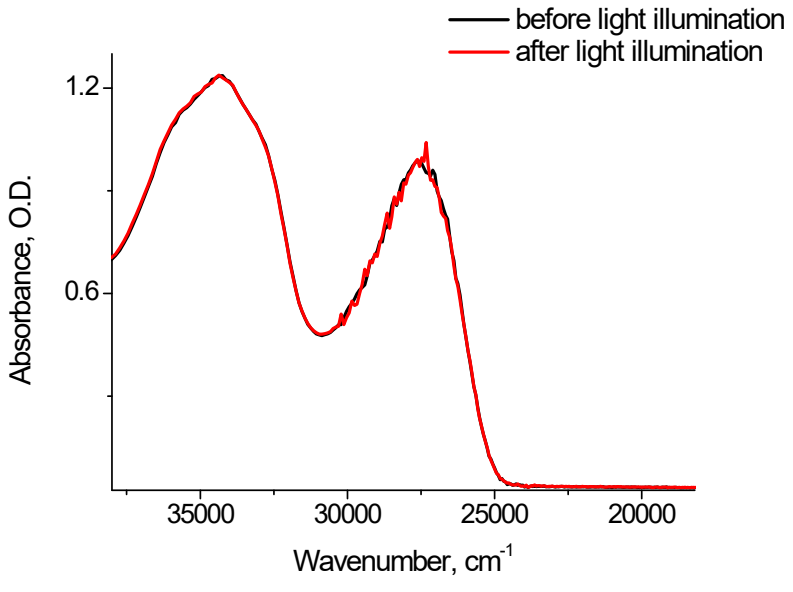

d

Figure S2. Photodamage test of **tBuTPAterpy**, exposed to 405 nm excitation in: chloroform (17 μW, 250 min) (a), acetonitrile (100 μW, 310 min) (b), glyceryl triacetate (110 μW, 310 min) (c), *n*-hexane (95 μW, 250 min) (d).

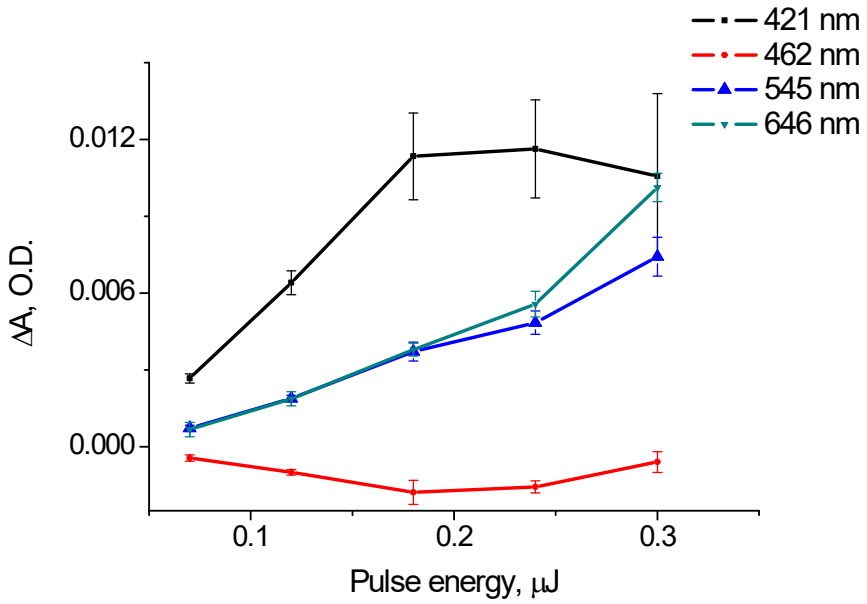
421 nm
462 nm
545 nm
646 nm
0.012
0.006
0.000
ΔA, O.D.
0.1
0.2
0.3
Pulse energy, μJ

a

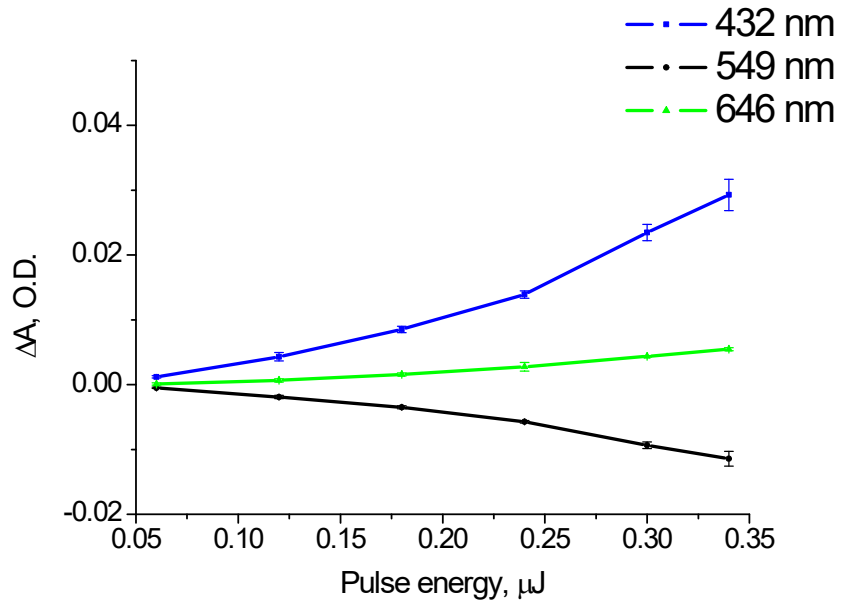
432 nm
549 nm
646 nm
0.04
0.02
0.00
-0.02
ΔA, O.D.
0.05
0.10
0.15
0.20
0.25
0.30
0.35
Pulse energy, μJ

b

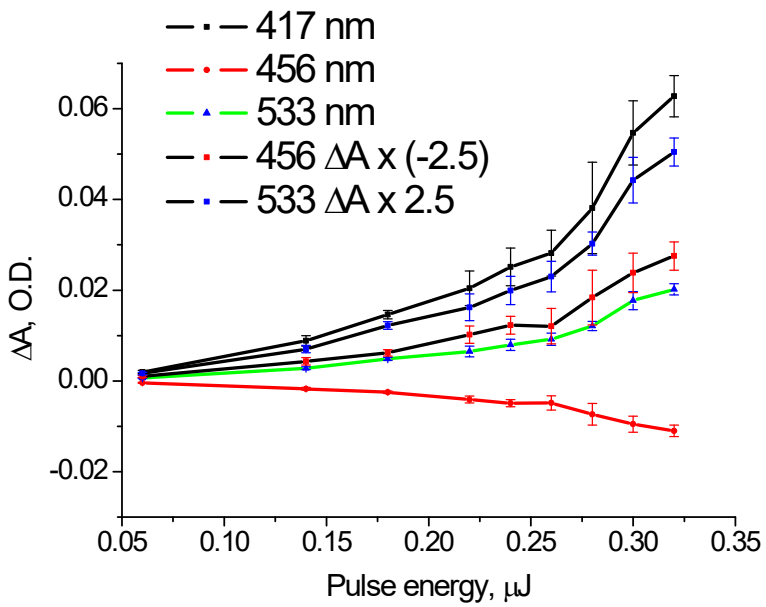

c

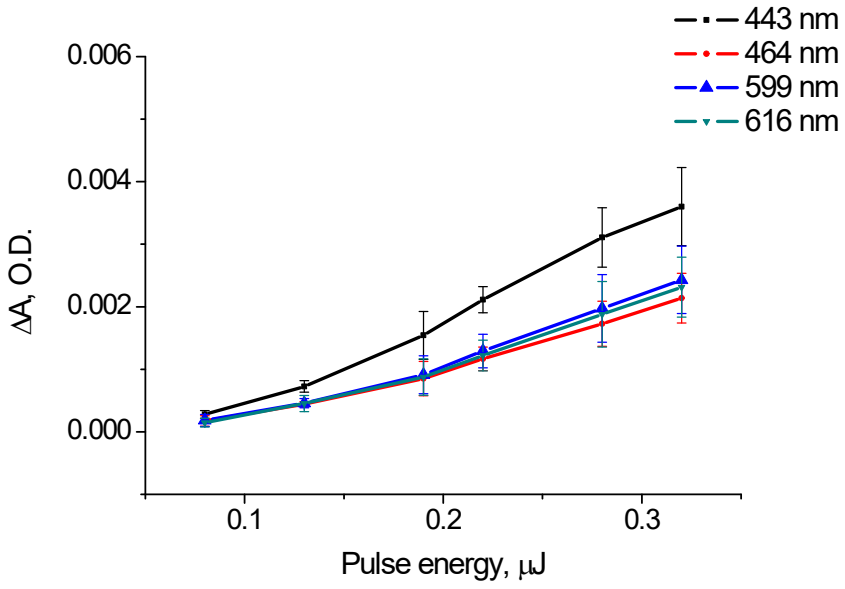

d

Figure S3. Fluence dependence for **tBuTPAterpy** in: chloroform (a), acetonitrile (b), glyceryl triacetate (c), *n*-hexane (d).

fs fluorescence upconversion measurements

Broadband femtosecond fluorescence upconversion (fsFlUC) measurements were collected using a setup consisting of a Ti:sapphire laser (Libra, Coherent), delivering 45 fs pulses centred at 800 nm with a repetition rate of 1 kHz, and a fluorescence spectrofluorimeter (LIOP- TEC) [2]. The generated beam centred at 800 nm was split in two, and ~25% of it was transmitted to a white light seeded optical parametric amplifier (OPerA-Solo, Coherent) to generate IR gate pulses of 1300 nm (110 μJ per pulse), while the rest of the signal was frequency-doubled in a I type of BBO crystal (d = 0.5 mm). The 400 nm pulses were used to excite the sample solution at the magic angle (54.7°). Most of the transmitted 400 nm light was blocked on a small beam stop and a 400 nm filter after passing through the sample position. Light upconversion was achieved by focusing both the fluorescence from the sample and the gate pulses onto a 100 μm thick BBO crystal (Eksma Optics). A type II sum-frequency generation is obtained from the horizontally polarized gate beam and the vertically polarized fluorescence. This is the most suitable configuration for upconversion of a broad frequency range. The phase-matching requirement and background-free detection of the signal were additionally supported by the large angle (21°) between the fluorescence and the gate beam. Then, the generated signal was focused by a concave mirror onto a fiber, while the frequency-doubled gate beam and the upconverted pump beam were blocked.

The light was collected via an unfolded Czerny-Turner spectrograph, including a UV-Vis grating, and detected by a CCD camera (Newton 920, Andor). The computer-controlled delay stage (PI) in the pump path allowed us to collect the upconverted fluorescence signal at different time delays with respect to the photoexcitation event. The full width at half maximum of the cross-correlation between the pump and probe pulses was used to estimate the instrument response function (IRF, equal to 0.140 ps and 0.150 ps, respectively, for $CHCl_3$ and acetonitrile solutions). The sample solutions (c = 250 μM) used in the FlUC experiments had an optical density of 0.3 – 0.5 at 400 nm (1 mm optical path quartz cuvettes) and was stirred with argon flow to avoid bleaching. For the global analysis of the FlUC data, the linear unidirectional sequential model of the Optimus™ [3] software was used.

fs TA measurements

The TA experiments were performed using a pump–probe transient absorption spectroscopy system (Ultrafast Systems, Helios). A regenerative amplified femtosecond Ti:sapphire laser system (Astrella, Coherent) delivered pulses of 100 fs duration with 5 mJ pulse energy at a repetition rate of 1 kHz and a central wavelength of 800 nm. The excitation pulses at 405 nm were generated from an optical parametric amplifier (Light Conversion, TOPAS prime). The white light continuum probe was generated by focusing the residual of the fundamental light into a CaF_2 crystal. The pump pulse was chopped by a mechanical chopper synchronised to one-half of the laser repetition rate and depolarised to mimic the dynamical changes of the orientation of the molecules. The delay time between the pump

and probe pulses was controlled with a delay line over a time scale up to 7.0 ns. For the detection of the transient absorption signals, the white light continuum passing through the sample was sent to a CCD detector installed in the system.

All TA experiments were carried out in solution using quartz cuvettes with a 2 mm path length. The solution concentration of 125 μM was selected in order to have an absorbance at the 405 nm pump wavelength in the range 0.25-0.5 O.D. During the experiments, sample damaging was prevented by stirring the solution.

TA data were initially processed using the Surface Xplorer (Ultrafast Systems) software and then analysed with use of the Optimus™ software [3]. Background correction, scattered light subtraction, solvent signal contribution subtraction and removal of spikes in the TA maps were routinely performed prior to the global lifetime analysis. The IRF and the white light chirp of the experiments were measured in the pure solvents (full width at half maximum, FWHM, of ~160fs, ~150fs, ~150fs, ~150fs respectively for $CHCl_3$, glyceryl triacetate, acetonitrile, *n*-hexane). The global analysis of the TA maps was performed using the linear unidirectional sequential model implemented in the Optimus™ software [3]. This analysis allowed the deconvolution of the transient spectra into evolution-associated spectra (EAS), providing the decay-associated spectra (DAS) as a linear combination of the EAS. Pump light scattering in the wavelength range 390 – 410 nm was excluded from the analysis.

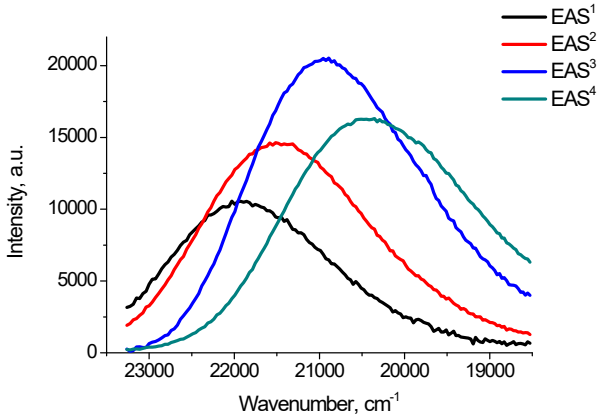
EAS1
EAS2
EAS3
EAS4
Intensity, a.u.
20000
15000
10000
5000
0
23000
22000
21000
20000
19000
Wavenumber, cm-1

A

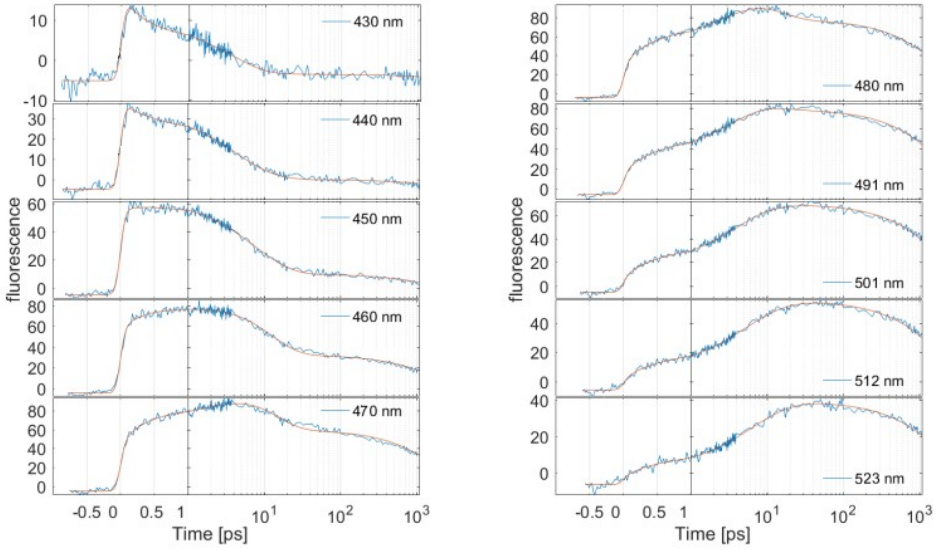
430 nm
440 nm
450 nm
460 nm
470 nm
480 nm
491 nm
501 nm
512 nm
523 nm
fluorescence
Time [ps]

B

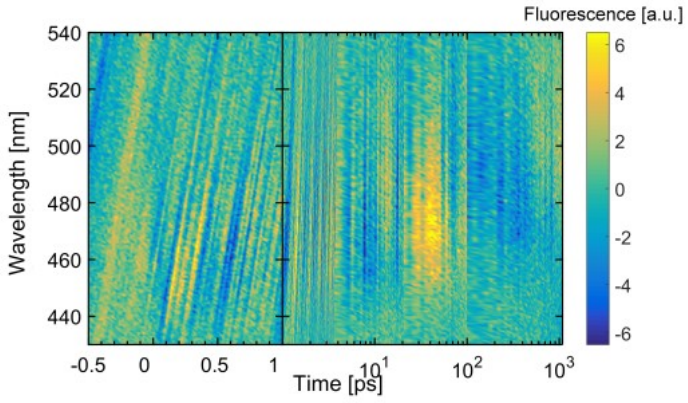
Fluorescence [a.u.]
Wavelength [nm]
Time [ps]

C

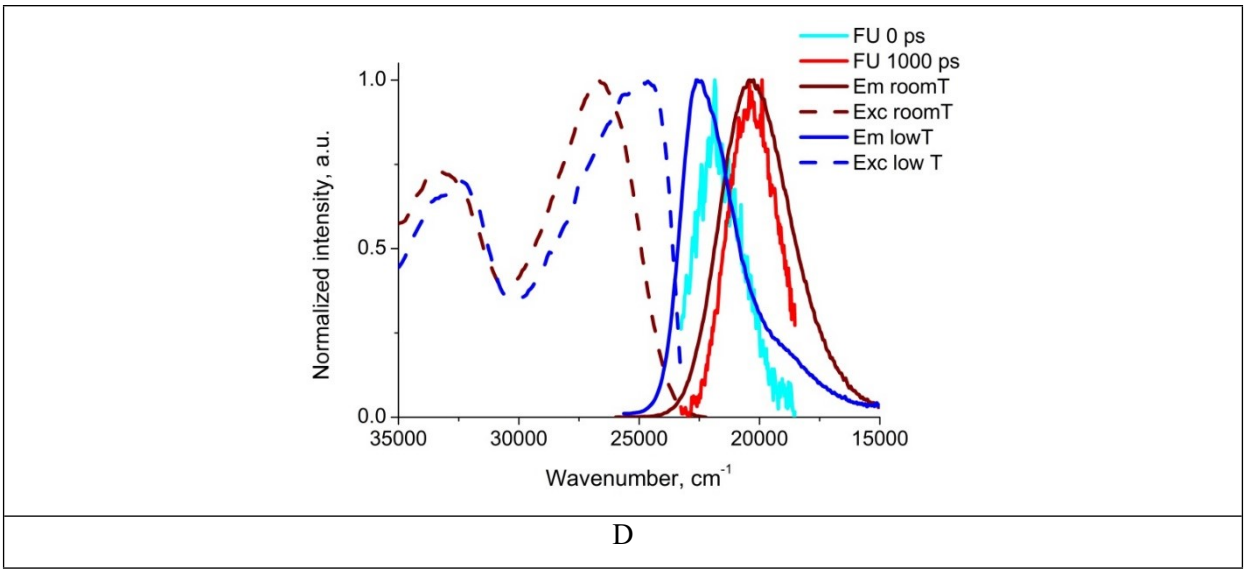

D

Figure S4. Evolution associated spectra (A), time traces and fitting curves obtained with the global analysis of the FlUC 2D maps (B) and the map of residuals (C) of **tBuTPAterpy** in $CHCl_3$. Comparison of steady-state emission (Em) and excitation (Exc) spectra at low (77 K) and room temperatures with the fluorescence upconverted (FU) signal at 0.2 ps and 1000 ps time delays (D).

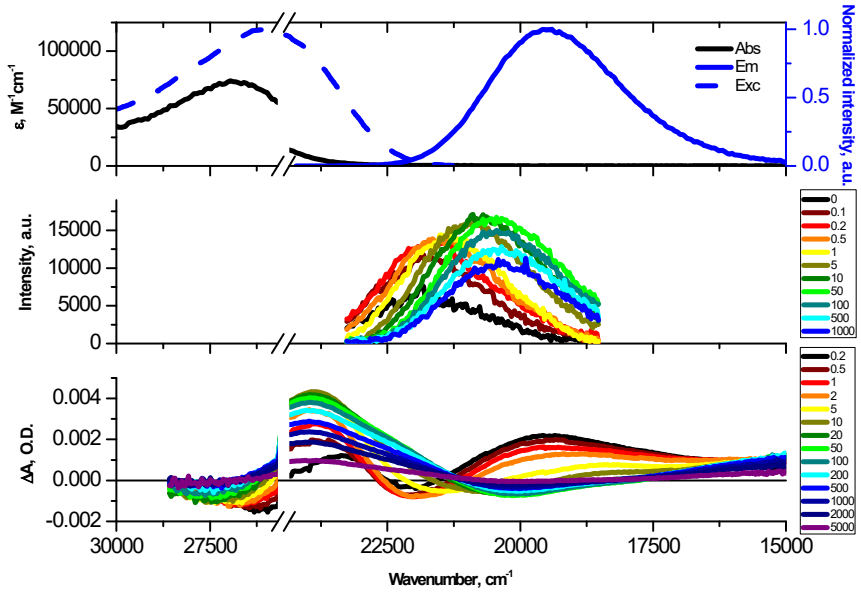

Figure S5. Comparison of absorption (Abs) [1], emission (Em) [1] and excitation (Exc) [1] spectra (top), FlUC spectra (middle) and TA spectra (bottom) of **tBuTPAterpy** in $CHCl_3$.

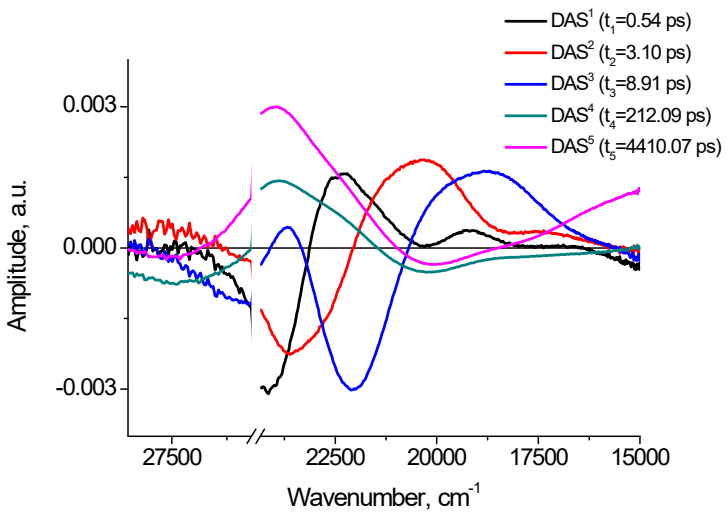
DAS1 (t1=0.54 ps)
DAS2 (t2=3.10 ps)
DAS3 (t3=8.91 ps)
DAS4 (t4=212.09 ps)
DAS5 (t5=4410.07 ps)
Amplitude, a.u.
0.003
0.000
-0.003
27500
22500
20000
17500
15000
Wavenumber, cm-1

A

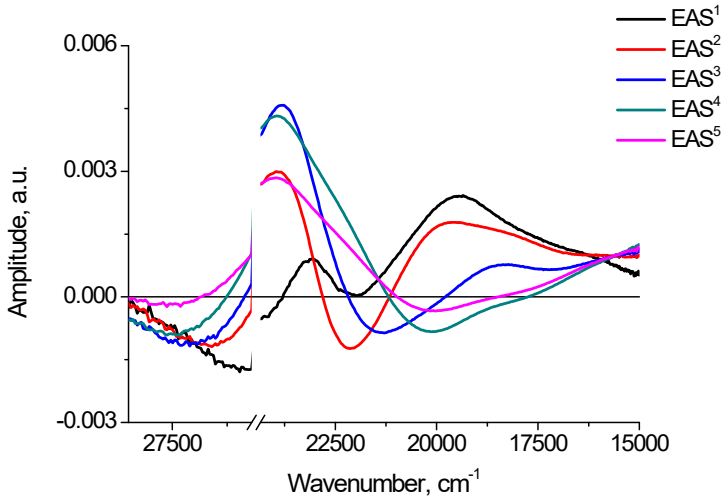
EAS1
EAS2
EAS3
EAS4
EAS5
Amplitude, a.u.
0.006
0.003
0.000
-0.003
27500
22500
20000
17500
15000
Wavenumber, cm-1

B

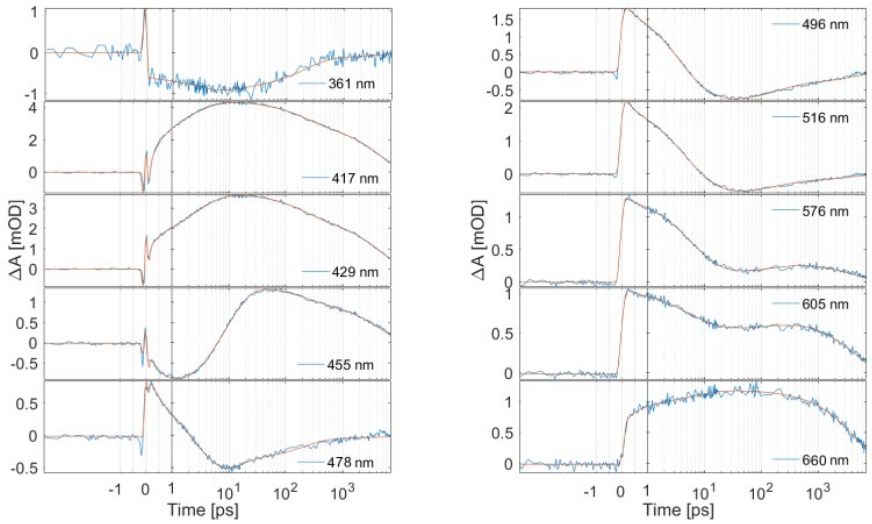
361 nm
417 nm
429 nm
455 nm
478 nm
496 nm
516 nm
576 nm
605 nm
660 nm
ΔA [mOD]
Time [ps]

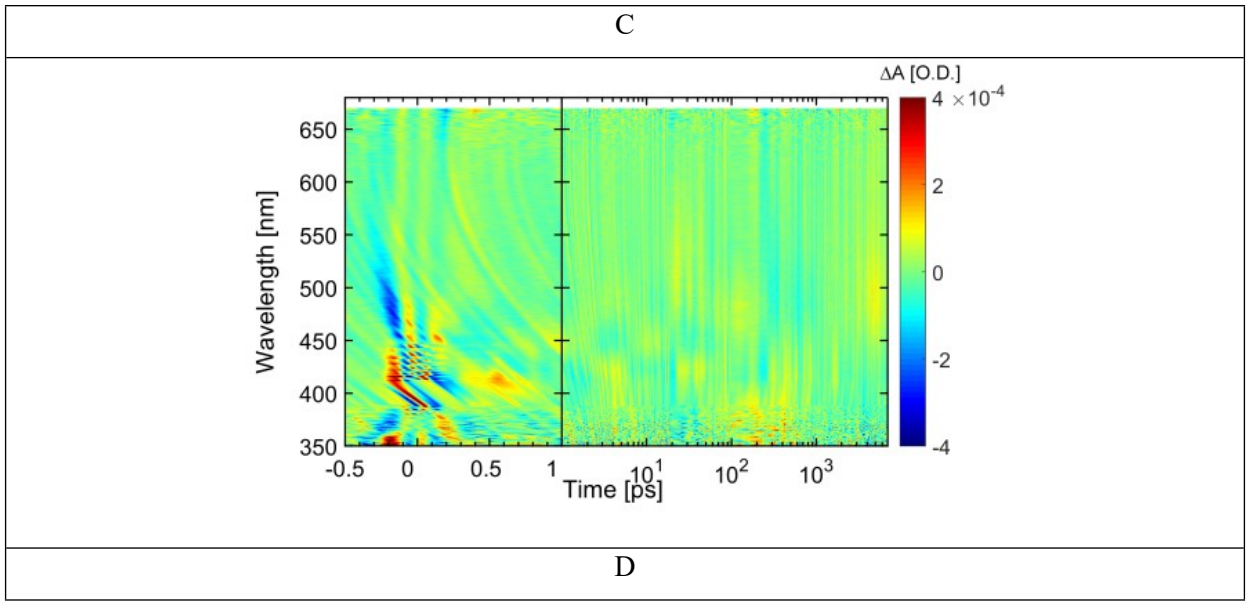

Figure S6. Decay associated spectra (A), evolution associated spectra (B), time traces and the fitting curves obtained from the global analysis of the TA 2D maps (C), and the map of residuals (D) of **tBuTPAterpy** in $CHCl_3$. The spectral range 395 – 410 nm was excluded from analysis due to pump light scattering.

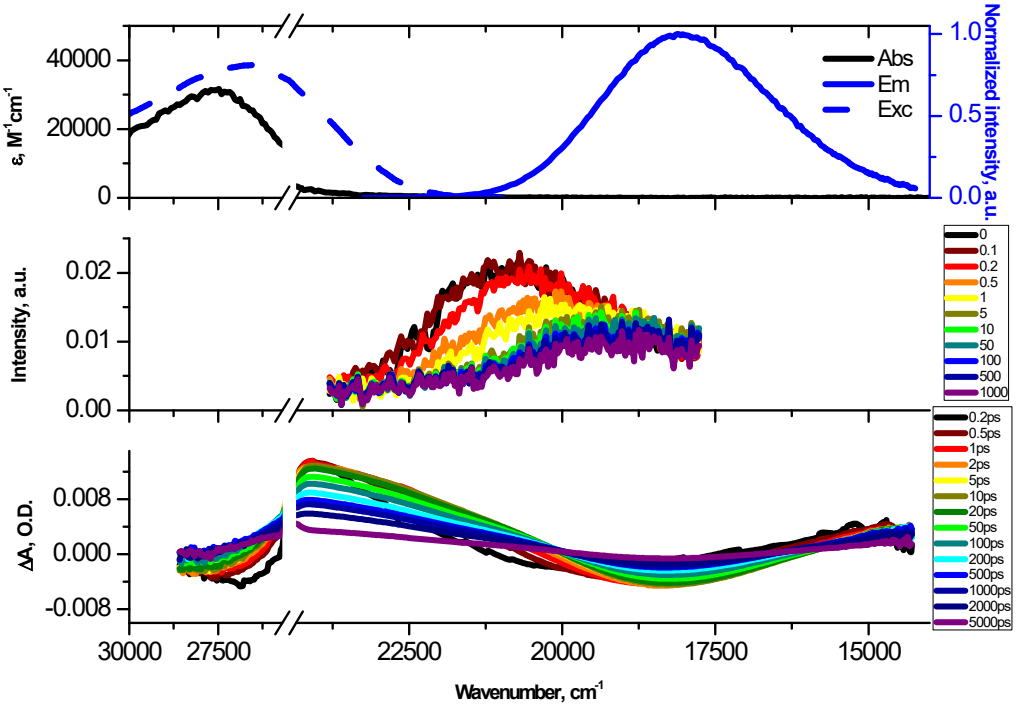

Figure S7. Comparison of FlUC, TA spectra and steady-state absorption (Abs) [1], emission (Em) [1] and excitation (Exc) [1] spectra of **tBuTPAterpy** in acetonitrile.

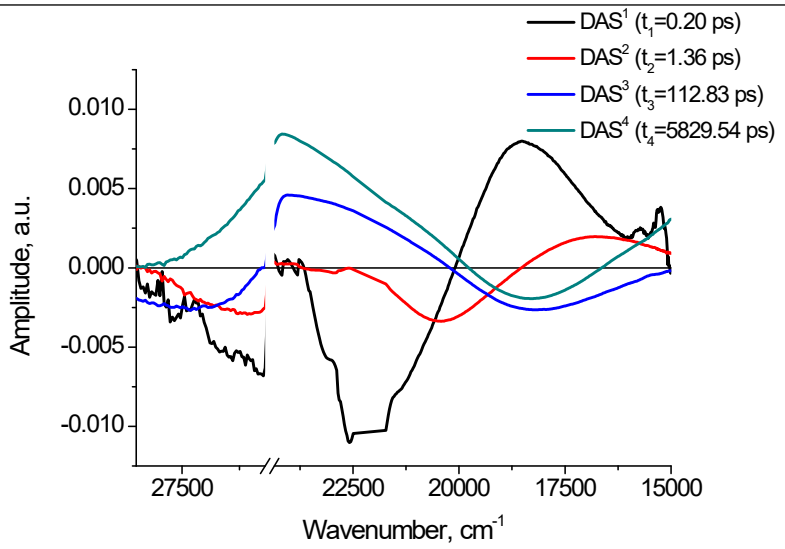
DAS1 (t1=0.20 ps)
DAS2 (t2=1.36 ps)
DAS3 (t3=112.83 ps)
DAS4 (t4=5829.54 ps)
Amplitude, a.u.
0.010
0.005
0.000
-0.005
-0.010
27500
22500
20000
17500
15000
Wavenumber, cm-1

A

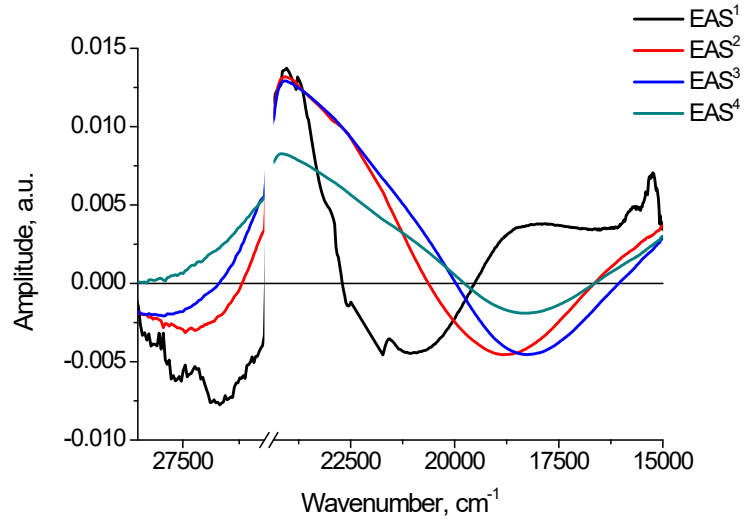
EAS1
EAS2
EAS3
EAS4
Amplitude, a.u.
0.015
0.010
0.005
0.000
-0.005
-0.010
27500
22500
20000
17500
15000
Wavenumber, cm-1

B

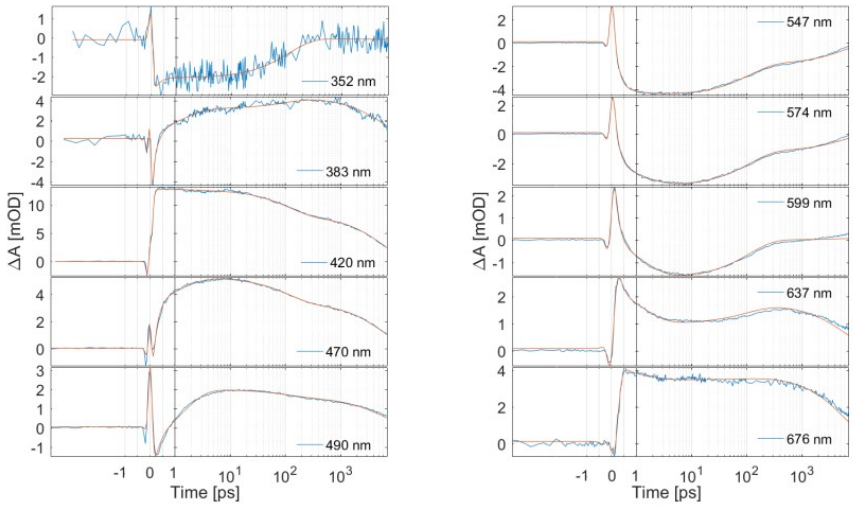
352 nm
383 nm
420 nm
470 nm
490 nm
547 nm
574 nm
599 nm
637 nm
676 nm
ΔA [mOD]
Time [ps]

C

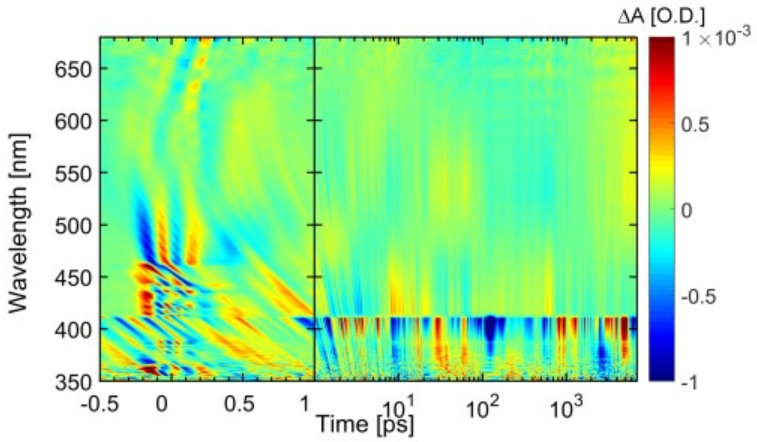

D

Figure S8. Decay associated spectra (A), evolution associated spectra (B), time traces and fitting curves obtained from the global analysis of the TA 2D maps (C) and the map of residuals (D) of **tBuTPAterpy** in acetonitrile. The spectral range 395 – 410 nm was excluded from analysis due to pump light scattering.

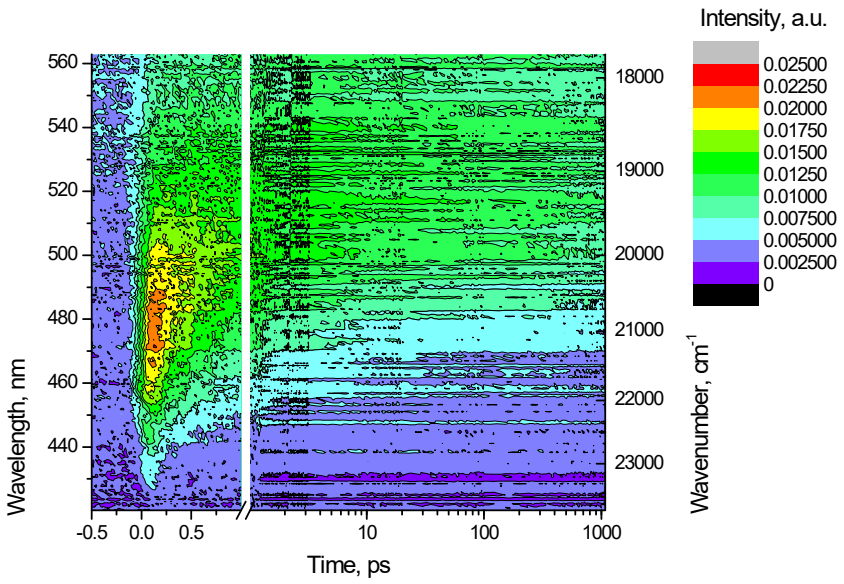
Intensity, a.u.
0.02500
0.02250
0.02000
0.01750
0.01500
0.01250
0.01000
0.007500
0.005000
0.002500
0
Wavelength, nm
560
540
520
500
480
460
440
-0.5
0.0
0.5
10
100
1000
Time, ps
18000
19000
20000
21000
22000
23000
Wavenumber, cm-1

A

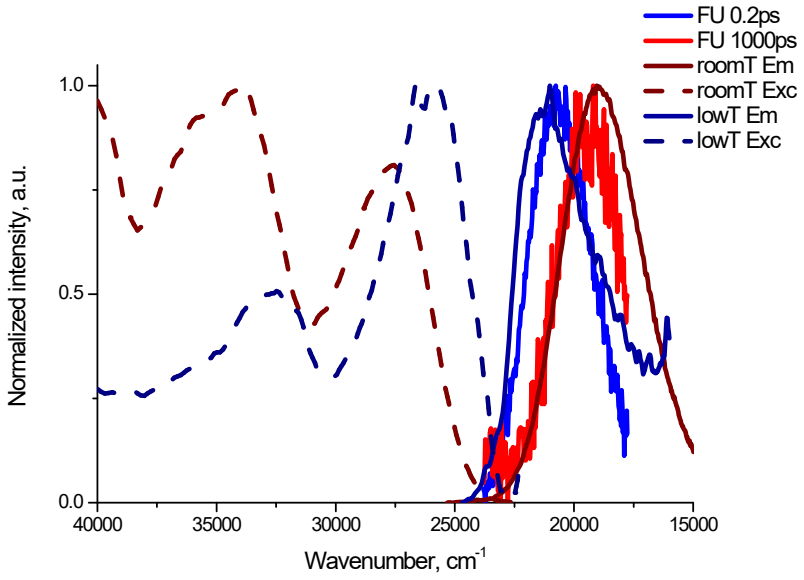
FU 0.2ps
FU 1000ps
roomT Em
roomT Exc
lowT Em
lowT Exc
Normalized intensity, a.u.
1.0
0.5
0.0
40000
35000
30000
25000
20000
15000
Wavenumber, cm-1

B

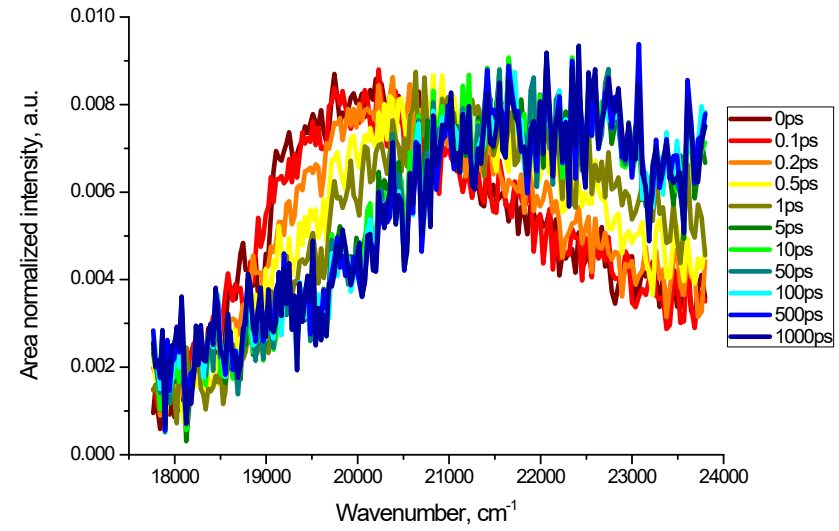

C

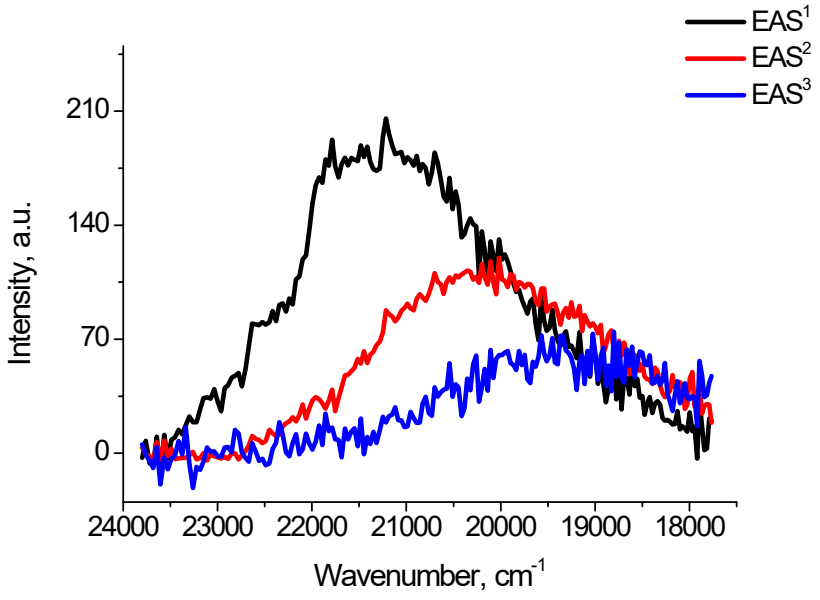

D

Figure S9. FlUC data for **tBuTPAterpy** in acetonitrile: FlUC 2D plot (A); comparison of steady-state emission (Em) and excitation (Exc) spectra at low (77 K) and room temperatures with the fluorescence upconverted (FU) signal at 0.2 ps and 1000 ps time delays (B); Time-resolved area normalized emission spectra (C); evolution associated spectra (D).

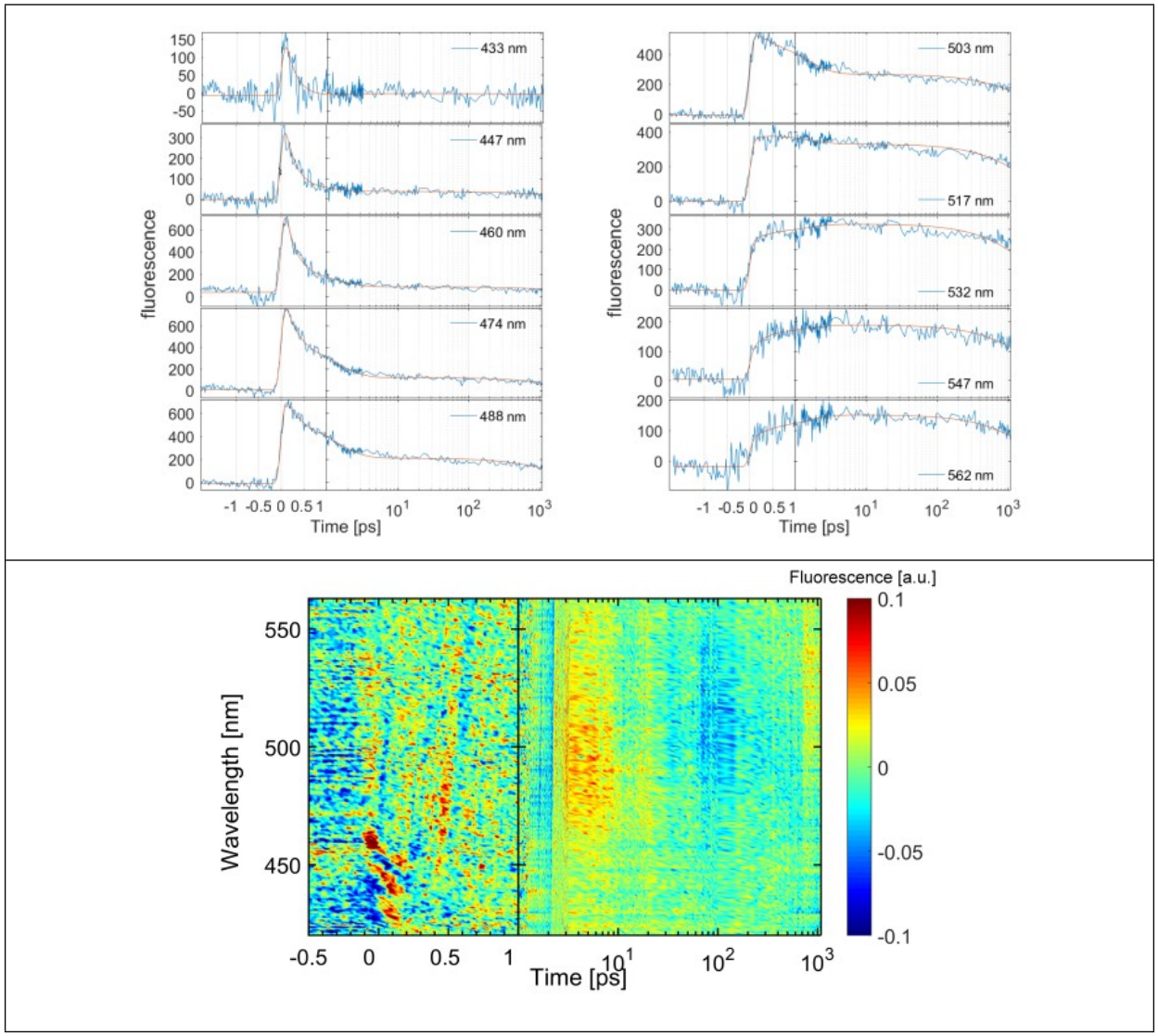

Figure S10. Time traces and the fitting curves obtained with the global analysis of the FlUC 2D maps (top) and the map of residuals (bottom) of **tBuTPAterpy** in acetonitrile. The spectral range 380 – 420 nm was excluded from the analysis due to pump scattering. The Raman scattering of the solvent was excluded from analysis.

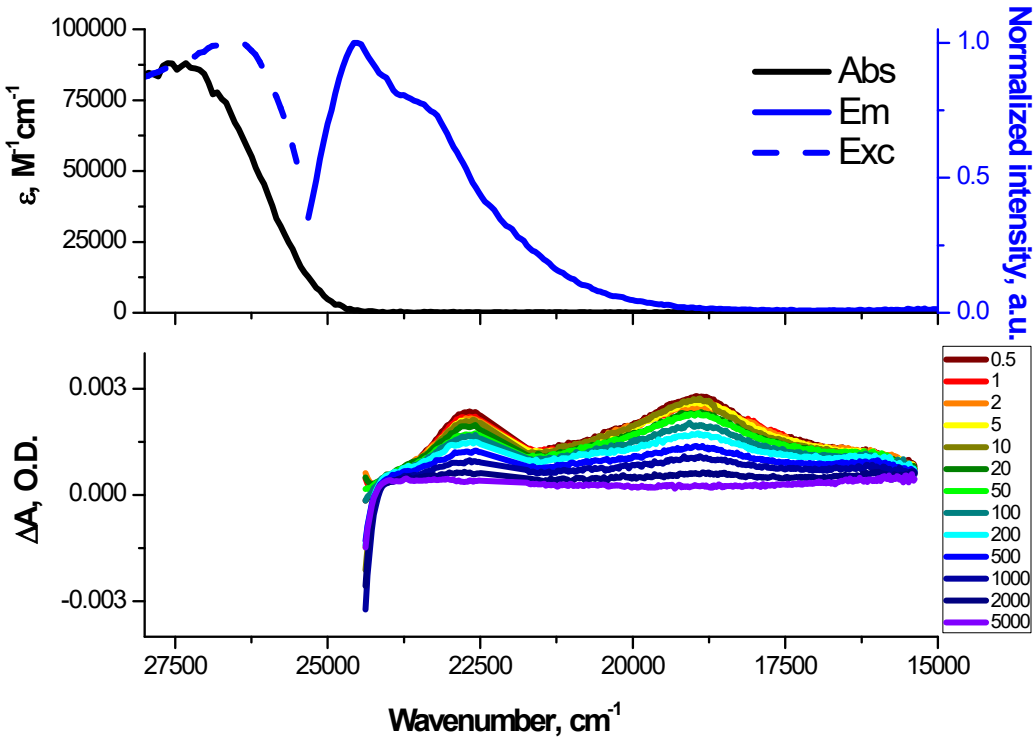

Figure S11. Comparison of TA spectra and steady-state absorption (Abs), emission (Em) and excitation (Exc) spectra of **tBuTPAterpy** in *n*-hexane.

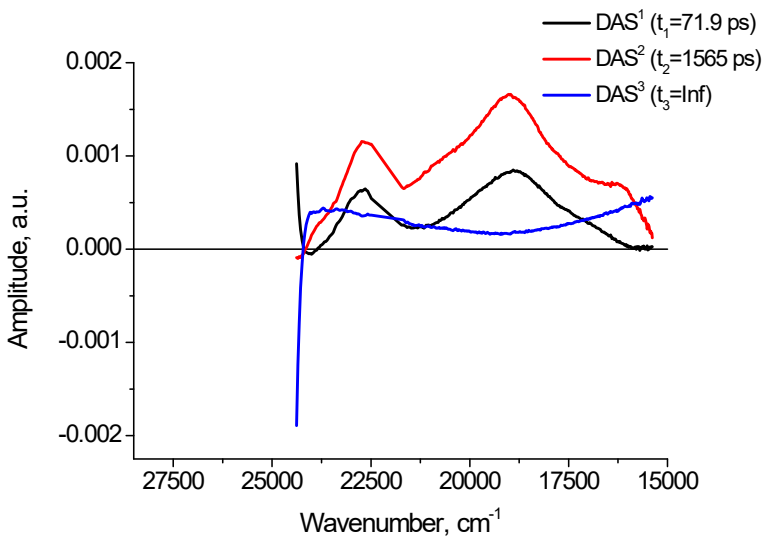
DAS1 (t1=71.9 ps)
DAS2 (t2=1565 ps)
DAS3 (t3=Inf)
Amplitude, a.u.
0.002
0.001
0.000
-0.001
-0.002
27500
25000
22500
20000
17500
15000
Wavenumber, cm-1

A

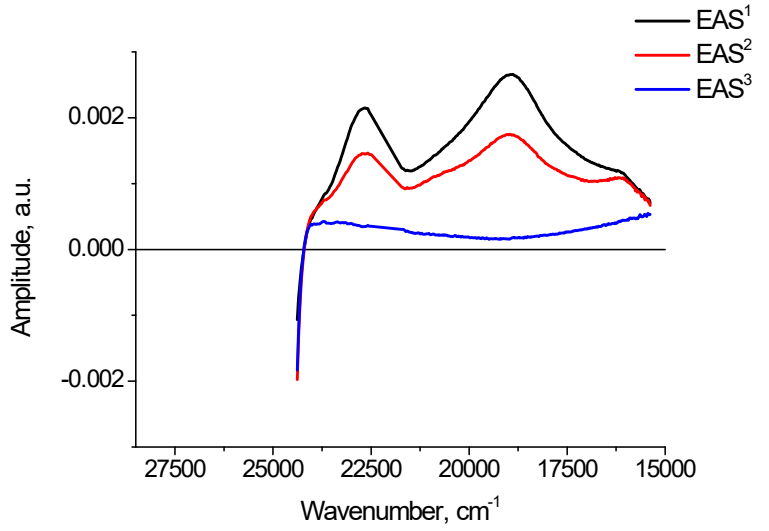
EAS1
EAS2
EAS3
Amplitude, a.u.
0.002
0.000
-0.002
27500
25000
22500
20000
17500
15000
Wavenumber, cm-1

B

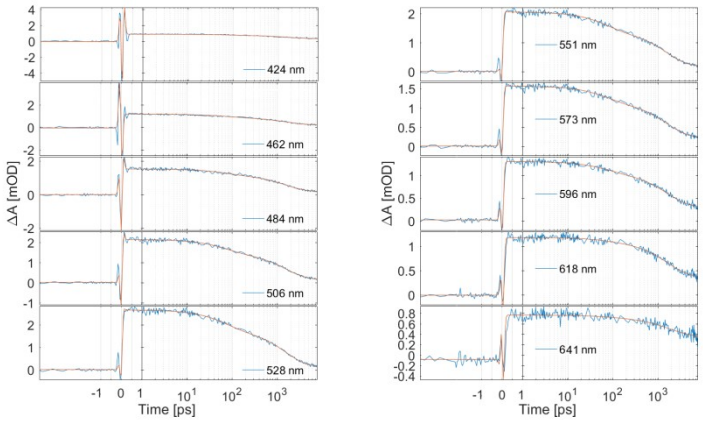
424 nm
462 nm
484 nm
506 nm
528 nm
551 nm
573 nm
596 nm
618 nm
641 nm
ΔA [mOD]
Time [ps]

C

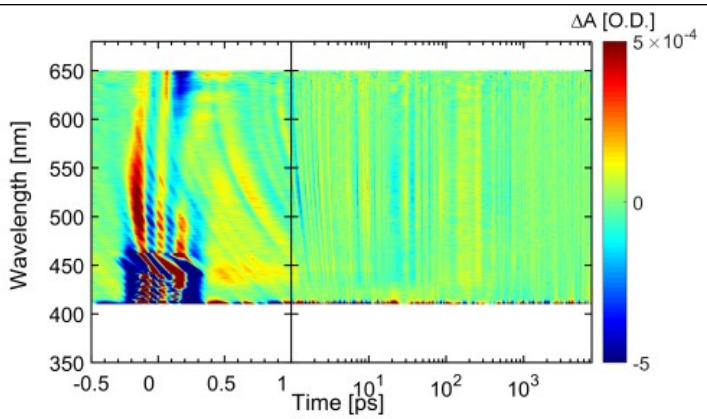

D

Figure S12. Decay associated spectra (A), evolution associated spectra (B), time traces and fitting curves obtained from the global analysis of the TA 2D maps (C) and the map of residuals (D) of **tBuTPAterpy** in *n*-hexane. Data in the range 445 – 460 nm containing the Raman scattering of the solvent were excluded from the analysis.

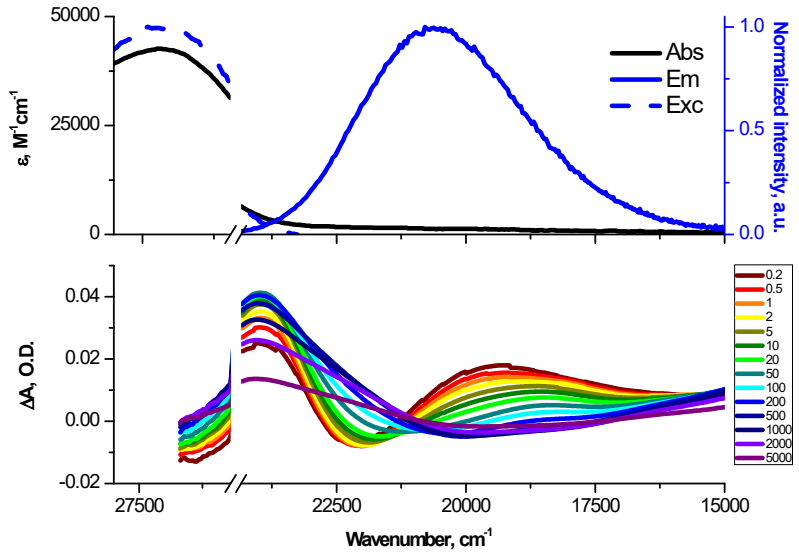

Figure S13. Comparison of steady-state absorption (Abs), emission (Em) and excitation (Exc) spectra (top) and TA spectra (bottom) of **tBuTPAterpy** in glyceryl triacetate.

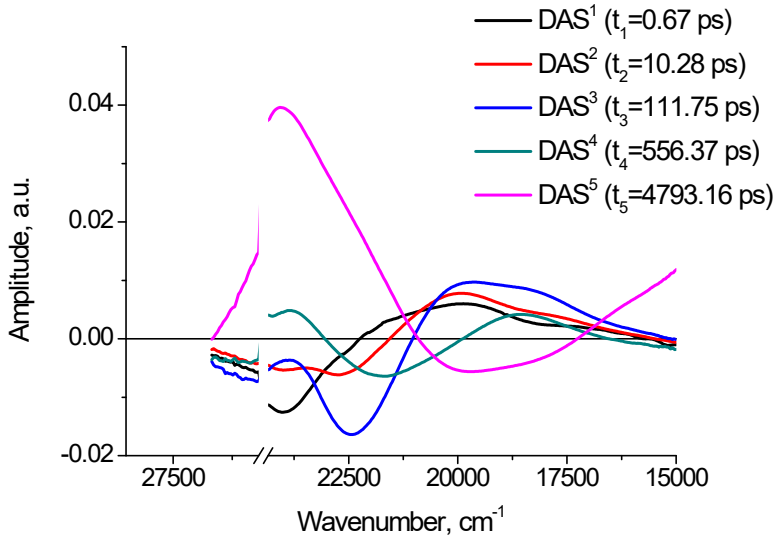
DAS1 (t1=0.67 ps)
DAS2 (t2=10.28 ps)
DAS3 (t3=111.75 ps)
DAS4 (t4=556.37 ps)
DAS5 (t5=4793.16 ps)
Amplitude, a.u.
0.04
0.02
0.00
-0.02
27500
22500
20000
17500
15000
Wavenumber, cm-1

A

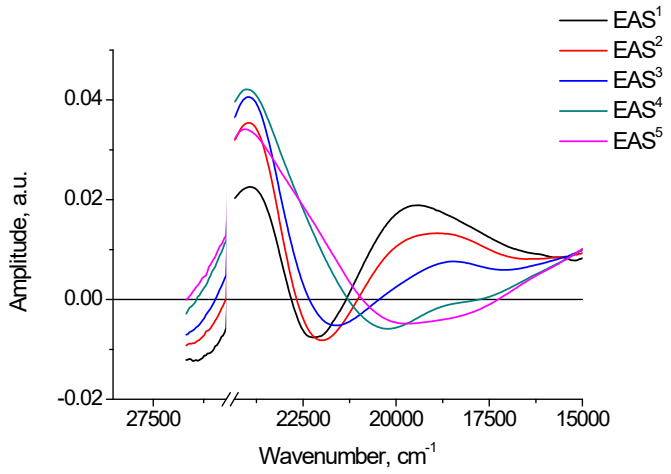
EAS1
EAS2
EAS3
EAS4
EAS5
Amplitude, a.u.
0.04
0.02
0.00
-0.02
27500
22500
20000
17500
15000
Wavenumber, cm-1

B

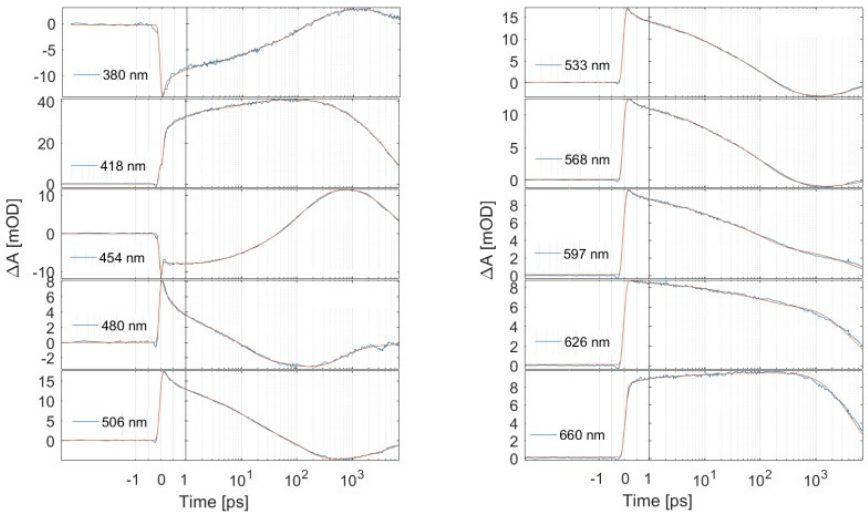
380 nm
418 nm
454 nm
480 nm
506 nm
533 nm
568 nm
597 nm
626 nm
660 nm
ΔA [mOD]
Time [ps]

C

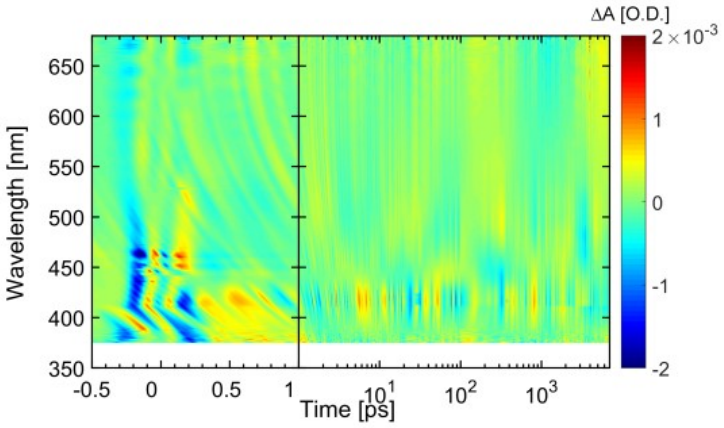

D

Figure S14. Decay associated spectra (A), evolution associated spectra (B), time traces and fitting curves obtained from the global analysis of the TA 2D maps (C) and the map of residuals (D) of **tBuTPAterpy** in glyceryl triacetate. The spectral range 395 – 410 nm was excluded from the analysis due to pump scattering.

<table>
<tr><td rowspan="2">3 comp</td><td> 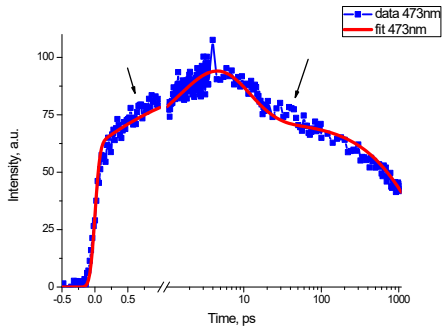
</td><td> 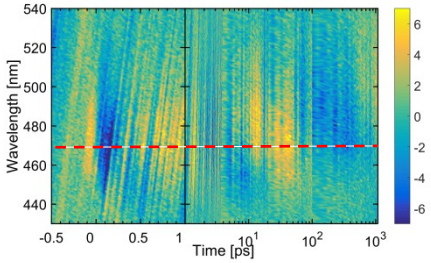
</td></tr>
<tr><td colspan="2">τ_1 = 2.08 ps, τ_2 = 9.17 ps, τ_3 = 1943.52 ps</td></tr>
<tr><td rowspan="2">4 comp</td><td> 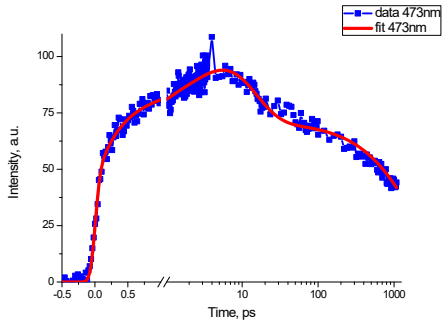
</td><td> 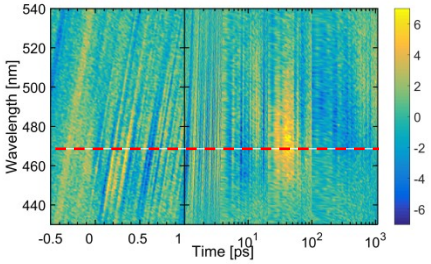
</td></tr>
<tr><td colspan="2">τ_1 = 0.31 ps, τ_2 = 3.72 ps, τ_3 = 9.75 ps, τ_4 = 2038.58 ps</td></tr>
<tr><td rowspan="2">5 comp</td><td> 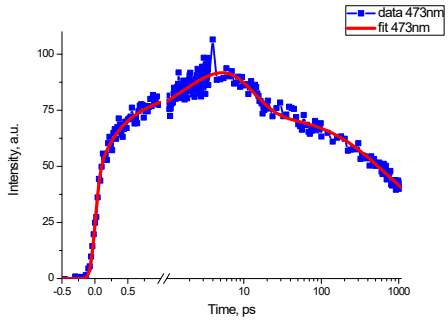
</td><td> 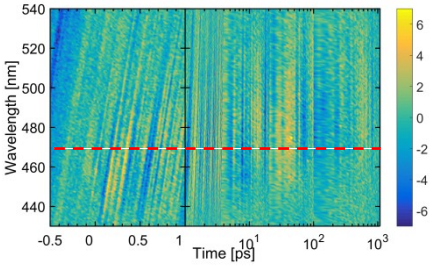
</td></tr>
<tr><td colspan="2">τ_1 = 0.29 ps, τ_2 = 3.32 ps, τ_3 = 7.95 ps, τ_4 = 391.30 ps, τ_5 = 4400.00 ps</td></tr>
</table>

Figure S15. Representative time traces (at 473 nm) and fitting curves obtained with an increasing number of time components in the global analysis of the FlUC 2D maps (left) and the map of residuals (right) of **tBuTPAterpy** in $CHCl_3$.

<table>
<tr><td>3
comp</td><td> 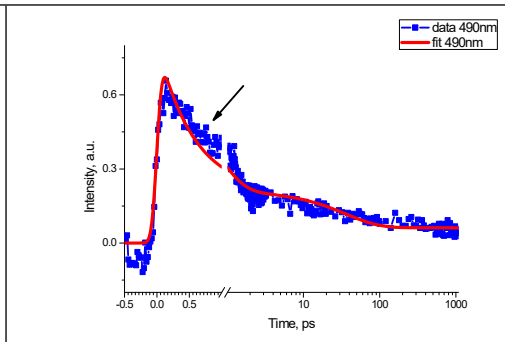
</td><td> 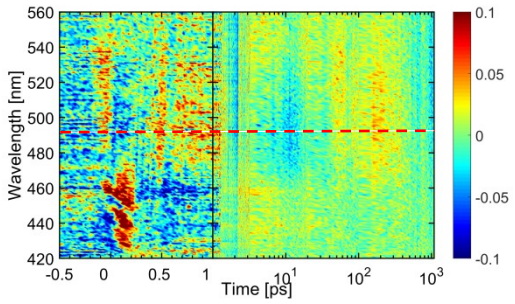
</td></tr>
<tr><td colspan="3">τ_1 = 0.56 ps, τ_2 = 36.44 ps, τ_3 = Inf</td></tr>
<tr><td>3
comp</td><td> 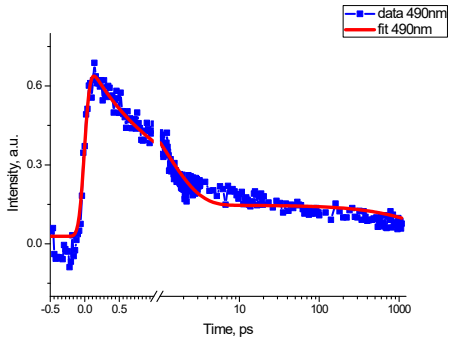
</td><td> 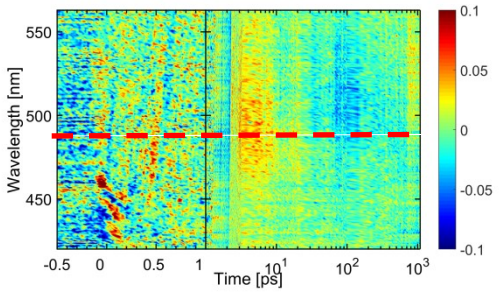
</td></tr>
<tr><td colspan="3">τ_1 = 0.23 ps (fixed), τ_2 = 1.21 ps, τ_3 = 2024ps</td></tr>
<tr><td>4
comp</td><td> 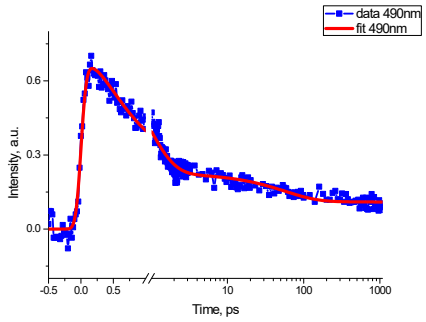
</td><td> 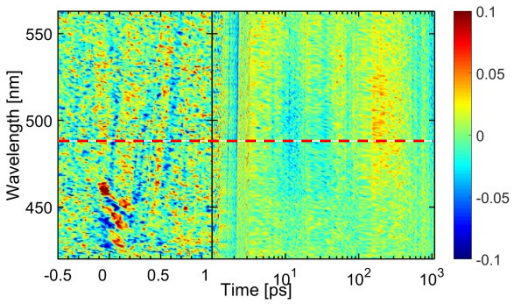
</td></tr>
<tr><td colspan="3">τ_1 = 0.23 ps, τ_2 = 0.67 ps, τ_3 = 57.48 ps, τ_4 = Inf</td></tr>
</table>

Figure S16. Representative time traces (at 490 nm) and fitting curves obtained with an increasing number of time components in the global analysis of the FlUC 2D maps (left) and the map of residuals (right) of **tBuTPAterpy** in acetonitrile.

<table>
<tr><td>3 comp</td><td> 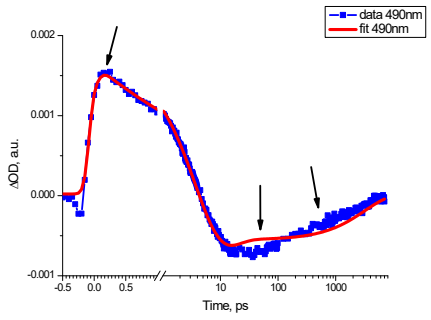
</td><td> 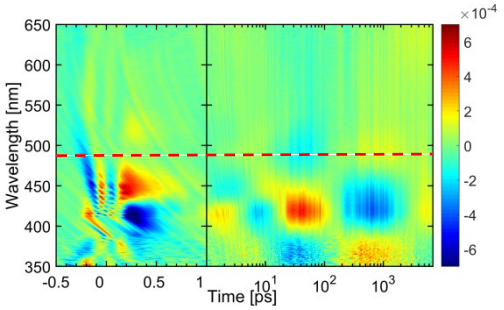
</td></tr>
<tr><td></td><td colspan="2">τ_1 = 4.23 ps, τ_2 = 8.27 ps, τ_4 = 3182.10 ps</td></tr>
<tr><td>4 comp</td><td> 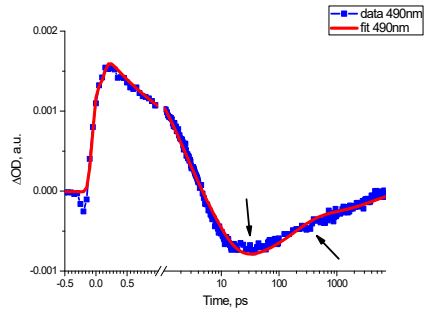
</td><td> 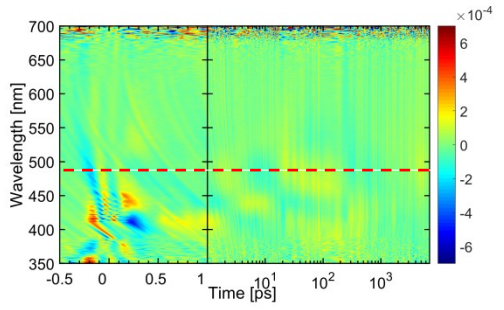
</td></tr>
<tr><td></td><td colspan="2">τ_1 = 1.39 ps, τ_2 = 7.31 ps, τ_3 = 179 ps, τ_4 = 4371.20 ps</td></tr>
<tr><td>5 comp</td><td> 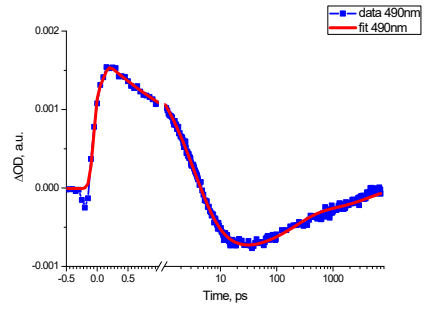
</td><td> 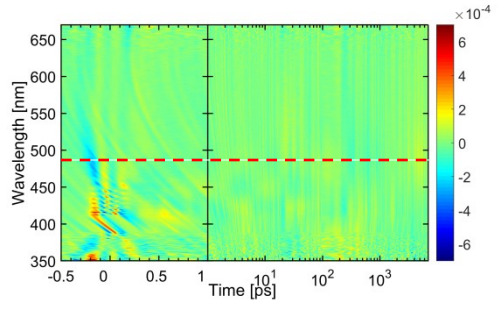
</td></tr>
<tr><td></td><td colspan="2">τ_1 = 0.54 ps, τ_2 = 3.10 ps, τ_3 = 8.91 ps, τ_4 = 212.08 ps, τ_5 = 4410.07 ps</td></tr>
</table>

Figure S17. Representative time traces (at 490 nm) and fitting curves obtained with an increasing number of time components in the global analysis of the TA 2D maps (left) and the map of residuals (right) of **tBuTPAterpy** in $CHCl_3$. The spectral range 395 – 410 nm was excluded from the analysis due to light scattering.

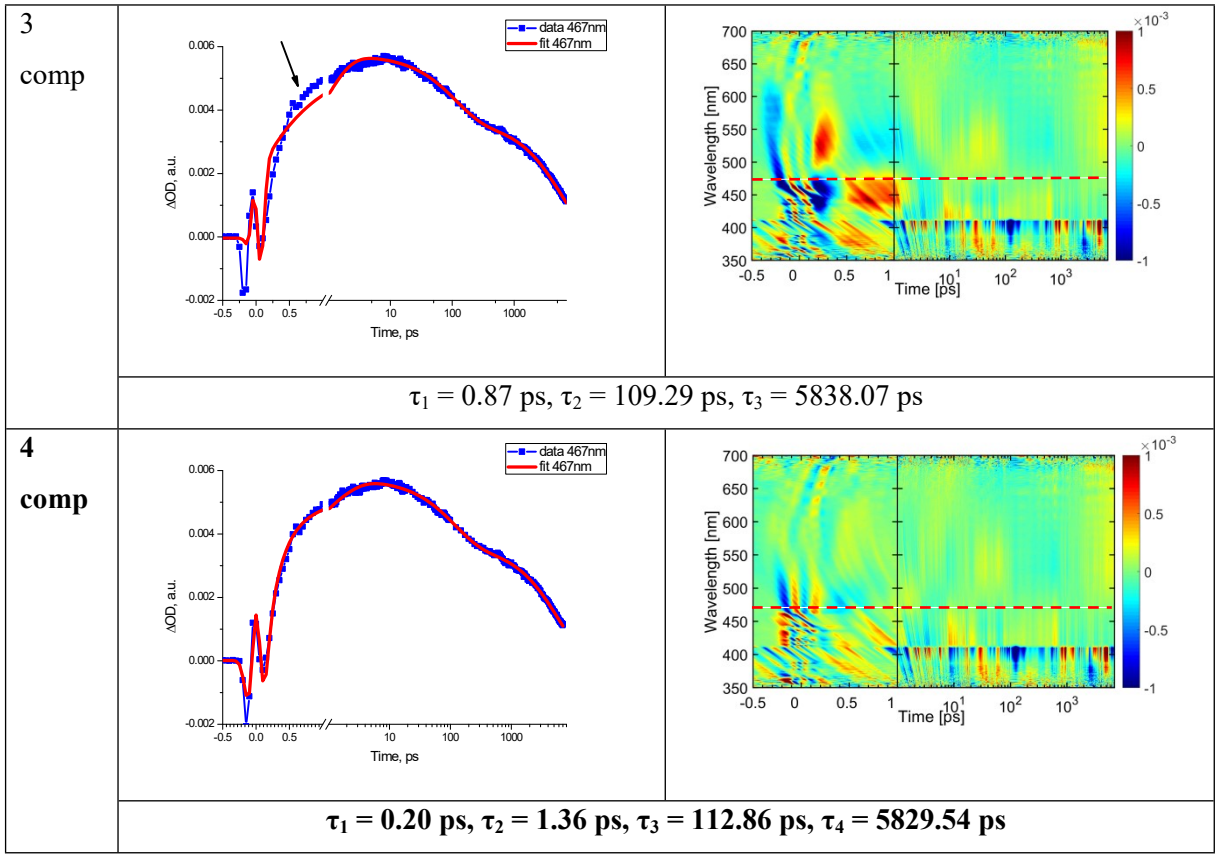

Figure S18. Representative time traces (at 490 nm) and fitting curves obtained with an increasing number of time components in the global analysis of the TA 2D maps (left) and the map of residuals (right) of **tBuTPAterpy** in acetonitrile. The spectral range 395 – 410 nm was excluded from the analysis due to light scattering.

2 comp	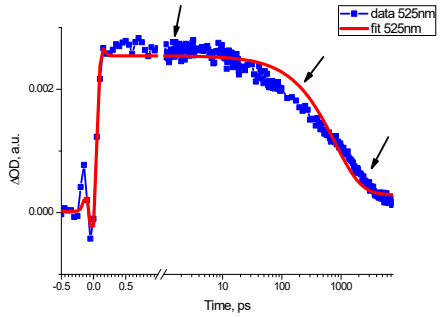	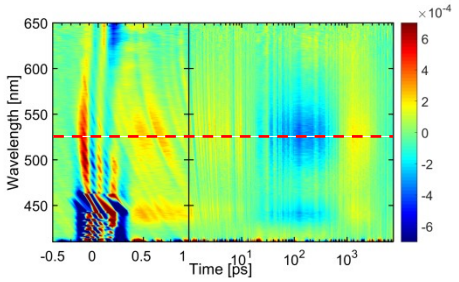
	τ_1 = 788.38 ps, τ_2 = Inf	
3 comp	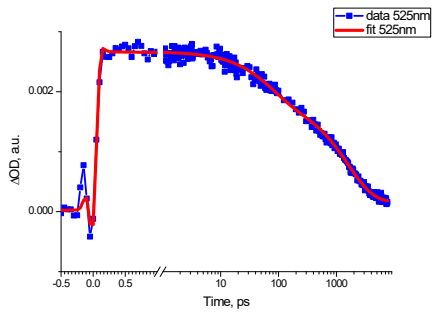	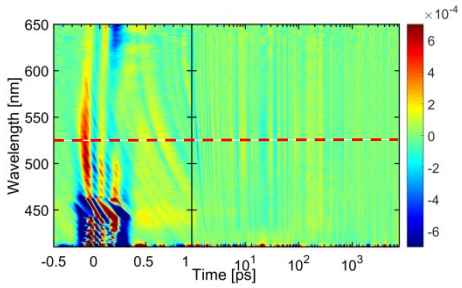
	τ_1 = 71.92 ps, τ_2 = 1565.31 ps, τ_3 = Inf	
4 comp	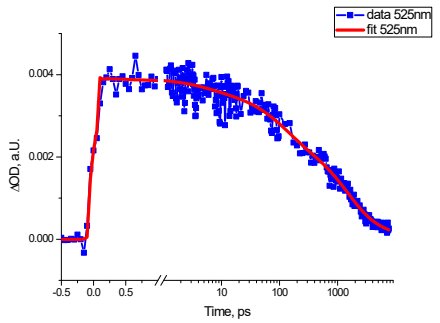	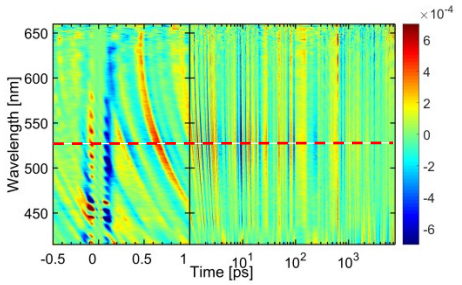
	τ_1 = 5.55 ps, τ_2 = 103.86 ps, τ_3 = 1356.38 ps, τ_4 = Inf	

Figure S19. Representative time traces (at 525 nm) and fitting curves obtained with an increasing number of time components in the global analysis of the TA 2D maps (left) and the map of residuals (right) of **tBuTPAterpy** in *n*-hexane. Data in the range 445 – 460 nm containing the Raman scattering of the solvent were excluded from the analysis.

3 comp	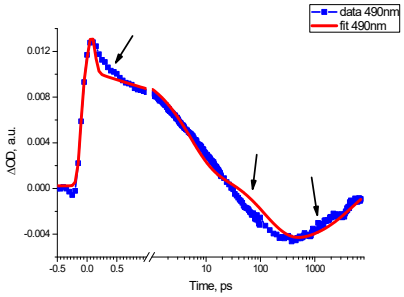	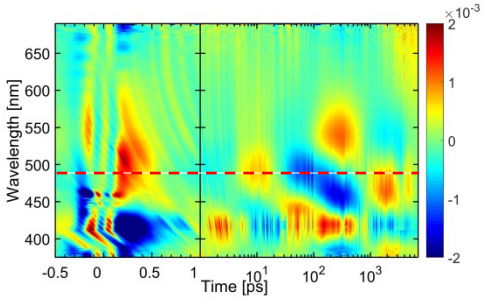
	τ_1 = 4.87 ps, τ_2 = 126.86 ps, τ_3 = 4746.37 ps	
4 comp	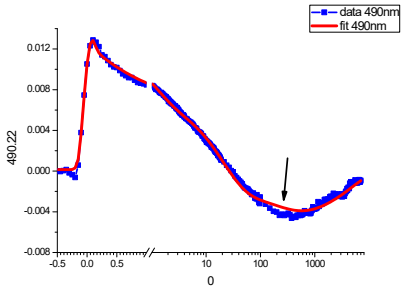	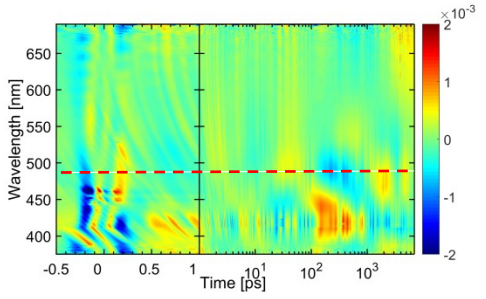
	τ_1 = 1.06 ps, τ_2 = 19.88 ps, τ_3 = 225.45 ps, τ_4 = 4702.88 ps	
5 comp	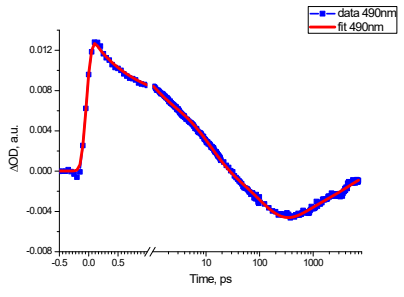	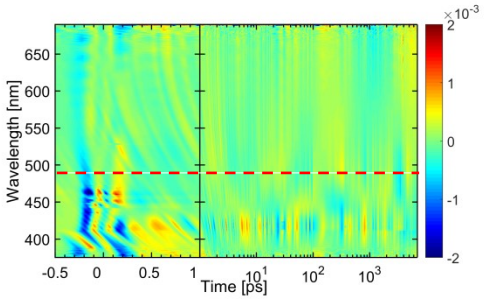
	τ_1 = 0.67 ps, τ_2 = 10.29 ps, τ_3 = 111.75 ps, τ_4 = 556.37 ps, τ_5 = 4793.16 ps	

Figure S20. Representative time traces (at 490 nm) and fitting curves obtained with an increasing number of time components in the global analysis of the TA 2D maps (left) and the map of residuals (right) of **tBuTPAterpy** in glyceryl triacetate. The spectral range 395 – 410 nm was excluded from the analysis due to pump light scattering.

References:

1. A. M. Maroń, A. Szłapa-Kula, M. Matussek, R. Kruszyński, M. Siwy, H. Janeczek, J. Grzelak, S. Mackowski, E. Schab-Balcerzak, B. Machura, Photoluminescence enhancement of Re(I) carbonyl complexes bearing D-A and D-π-A ligands, *Dalton Transactions*, **2020**, *49*, 4441-4453

2. E. Socie, B. R. C. Vale, A. Burgos-Caminal, J.-E. Moser, Direct Observation of Shallow Trap States in Thermal Equilibrium with Band-Edge Excitons in Strongly Confined CsPbBr3 Perovskite Nanoplatelets. *Advanced Optical Materials*, **2021**, *9*, 2001308

3. C. Slavov, H. Hartmann, J. Wachtveitl, Implementation and Evaluation of Data Analysis Strategies for Time-Resolved Optical Spectroscopy. *Anal. Chem.*, **2015**, *87*, 2328–2336

4. A. M. Maroń, O. Cannelli, E. C. Socie, P. Lodowski and B. Machura, Push-Pull Effect of Terpyridine Substituted by Triphenylamine Motive—Impact of Viscosity, Polarity and Protonation on Molecular Optical Properties, *Molecules*, 2022, **27**, 7071.